Organic Electronics 14 (2013) 2564–2572

Contents lists available at SciVerse ScienceDirect

Organic Electronics

journal homepage: www.elsevier.com/locate/orgel

Selective charge transfer in donor/acceptor systems bridged by Tröger base derivatives

Cristina L. Ramírez [a], Raúl Procaccini [b], Carlos A. Chesta [c], Alejandro R. Parise [a,*], D. Mariano A. Vera [a,*]

[a] Departamento de Química, Facultad de Ciencias Exactas y Naturales, Universidad de Mar del Plata, Funes 3350, B7602AYL Mar del Plata, Argentina
[b] INTEMA, Facultad de Ingeniería, Universidad Nacional de Mar del Plata, Av. Juan B. Justo 4302, B7608FDQ Mar del Plata, Argentina
[c] Departamento de Química, Facultad de Ciencias Exactas Físicoquimicas y Naturales, Universidad Nacional de Rio Cuarto, 5800 Las Higueras, Argentina

ARTICLE INFO

Article history:
Received 19 April 2013
Received in revised form 20 June 2013
Accepted 22 June 2013
Available online 10 July 2013

Keywords:
Donor/acceptor dyads
Intramolecular electron transfer
Intervalence
CAM-B3LYP
OLEDS
DSSC

ABSTRACT

Recently, unusual charge transfer properties of two triarylamines bridged through an aliphatic bridge (Tröger base) have been reported. The donor/acceptor couple was shown to have an important electronic coupling between its centers for the *hole* transfer, although in the absence of a π linker. In contrast, we here show, by combining first principles calculations with experimental studies, that the bridge has a practically null role in coupling the *electron* transfer. This sharp contrast might present an interesting potential in the design of molecular devices.

1. Introduction

Due to its well-developed synthetic chemistry [1], triarylamines have turned into a family of versatile molecules capable of being used in the manufacture of light-current energy conversion devices, among other technological uses. They have found broad applications not only in OLEDs displays (where electrons and holes recombination results in efficient, molecular-based illumination devices) [2] but also in the design of dye sensitized solar cells (DSSCs). In the latter devices, light absorption generates a hole-electron pair (usually connected between them by a π linker) that either recombines or induces the charges to migrate in opposite directions (the hole being transferred to the electrolyte and the electron to a semiconductor). Also in these cases, the efficiency is determined by the proper design of the molecular device, which in turn requires a deep knowledge of the primary charge transfer processes [3–5]. Besides their promising roles in electro-optical or optical-electric transducers, triarylamines are also regarded as possible building blocks of molecular electronic devices. However, there are just a few basic studies regarding charge transfer processes between them [6]. Interestingly, in most relevant environments, the charge transfer processes are either through-space mediated (hoping) or through the bonds of a π system (other polymeric and/or discrete devices) [2]. Again the description at molecular level of these primary processes is valuable since it would shed light for designing building blocks for electronic arrays on rational bases, either as materials or as single molecular devices.

We have recently proved that an aliphatic Tröger base derivative acts as a very efficient bridge between triarylamine redox centers to a such extent that it can be compared to typical π bridges, although the bridge is an aliphatic fragment [7]. These findings are interesting *per se*, and they could be applied in devices connecting redox centers other than triarylamines. Besides, the bridge is also

* Corresponding authors.
E-mail addresses: aparise@mdp.edu.ar (A.R. Parise), dmavera@yahoo.com (D.M.A. Vera).

1566-1199/$ - see front matter © 2013 Elsevier B.V. All rights reserved.
http://dx.doi.org/10.1016/j.orgel.2013.06.024

curved ("V"-shaped), fact which could be exploited as a desirable feature for designing rod dyads for DSSCs [8–10]; in addition, its shape could avoid the π stacking which deactivates the emission in solid phase [11,12]. However, probably the most important feature of the Tröger base bridges was not uncovered previously, in oxidation (hole transfer) conditions. Here we show that this bridge might present the interesting potential of being a smart bridge, in the sense that it can selectively transport a hole but not an electron, in given conditions. This behavior would certainly open new possibilities for the design of novel devices.

This work aims to prove this hypothesis by means of a theoretical and experimental study of compounds **A–G** (Scheme 1). Tritolylamine (**TTA**) was used as reference redox potential experimentally as well as theoretically. In our previous work, **A** was synthesized, its hole transport properties were studied and it will now be tested in conditions of electron transport. **B** was also synthesized by us and used as the simplest model of an aliphatic bridge with weak electronic coupling [13,14]. **C** was experimentally studied in Ref. [15] in conditions of oxidation. Besides the experimental information regarding **C** [15], it is used as an example of a Robin and Day's Class III, delocalized, highly coupled intervalence system (and a typical π-mediated donor/acceptor dyad for either hole or electron transport) [16,17].[1] Compounds **D–E** are easier to reduce than **A** and they were used for probing the electron transport features of the bridge; **F–G** were used for comparison purposes and validation of the theoretical methodology. (The substance characterization of some of them, specifically synthesized for these studies, are available as part of the Electronic Supplementary Material, SM).

2. Materials and methods

2.1. Compounds under study

TTA used for the electrochemical studies was purchased from Aldrich and used as received. Compound **A** was used in Ref. [7] in conditions of oxidation and here its reduced species is only calculated theoretically. Preparation and characterization of **B** was already described [13,14]. Compounds **D** and **E** and their radical ions were characterized by first principles calculations and **E** was chosen for synthesis. It was prepared following the recommendations of Lutzen et al. [18]. The remaining compounds were synthesized in Butchwald–Hartwig conditions. The synthesis of **F** and **G** is summarized on Scheme 2.

A solution of 2,8-di-bromo-10,4-dimethyl-6H, 12H-5,11-methanodibenzo[b,f][1,5]-diazocine (0.01 mol), diarylamine (0.01 mol), $CsCO_3$ (0.015 mol), palladium acetate (5%) and [(*t*-Bu)$_3$PH]BF_4 (5%) in toluene (15 ml) was heated at reflux for 15 h. The reaction mixture was filtered and the solvent volume reduced *in vacuo*. The crude mixture was purified by silica column chromatography and the solvent mixture was *n*-hexane/ethyl acetate (2–5%). Full details about the substance characterization of the novel compounds are available as SM, Part 2.

2.2. Electrochemical characterization

The potentials obtained for $\mathbf{A}^{\cdot+}/\mathbf{A}$, $\mathbf{B}^{\cdot+}/\mathbf{B}$, $\mathbf{E}/\mathbf{E}^{\cdot-}$, $\mathbf{F}^{\cdot+}/\mathbf{F}$, $\mathbf{G}^{\cdot+}/\mathbf{G}$ and $\mathbf{TTA}^{\cdot+}/\mathbf{TTA}$ couples were obtained from cyclic voltammetry in a Teq-02 potentiostat using a conventional tree-electrode cell. Dry dichloromethane was used as electrolysis solvent and $TBAPF_6$ 0.05 M as supporting electrolyte. The working electrode was a 50 μm diameter platinum disc (99.99% purity) exposed from a 50 μm platinum wire sealed in glass tube. A plate of 99.9% gold was used as counter electrode. A wire of Ag was used as reference electrode and standardized using ferrocene/ferrocenium couple in dichloromethane [19]. The platinum electrode was polished with 1% w/w alumina powder (1 mm) in water over a piece of cloth, cleaned in an ultrasonic bath with absolute ethanol and dried in air. All the potentials reported in Table 1 are relative to the $\mathbf{TTA}^{+}/\mathbf{TTA}$ couple [7,20], i.e. the differences in the standard potential with respect to that reference reduction.

2.3. Spectroelectrochemistry

Spectroelectrochemistry experiments were performed in a four-electrode quartz thin layer cell using a graphite felt counter electrode, platinum woven wire working electrode (70 μm wires), a silver pseudoreference and an additional small platinum electrode to measure cyclic voltammograms prior to the electrolysis. Electronic spectra were measured using a Shimadzu UV160-U and a Shimadzu UV-3101PC spectrophotometers.

3. Theoretical calculations

The general setup for the first principles calculations was similar to that of Ref. [7]. The optimized structures of all compounds were obtained by full geometry optimization in gas phase and in dichloromethane as model solvent, using CAM-B3LYP and 6-31+G* [7]. In all cases, the SCRF model IEFPCM was used for simulating the solvation effect [21–26]. The nature of minima of the stationary point was checked by means of the analysis of the harmonic frequencies also in the model solvent with 6-31G* bases. The calculated values of the shifts in the potentials of Table 1 were referred to the $\mathbf{TTA}^{\cdot+}/\mathbf{TTA}$ couple. The thermodynamic cycles are described in previous works [7,20]. The contributions to the overall shifts (from the electron affinities or ionization potential and the free energies of solvation of charged and neutral species) are summarized in SM Table S1.

For the estimation of the vertical excited states in dichloromethane a TD-DFT approach was used [7,27,28].

[1] Typical π bridges mostly used in these technological applications are efficient for coupling either electron, hole or exciton transfer. In this case, due to the simplicity of the π link there is no reason to expect a different behavior. However and despite this general trend, there are some interesting exceptions. Sometimes, a π bridge could –by certain orbital symmetry control– allow for a poor coupling. Two interesting examples, among others, are one reversible electron transfer system (intervalence electron transfer) in Ref. [16] and one irreversible (dissociative electron transfer) in Ref. [17].

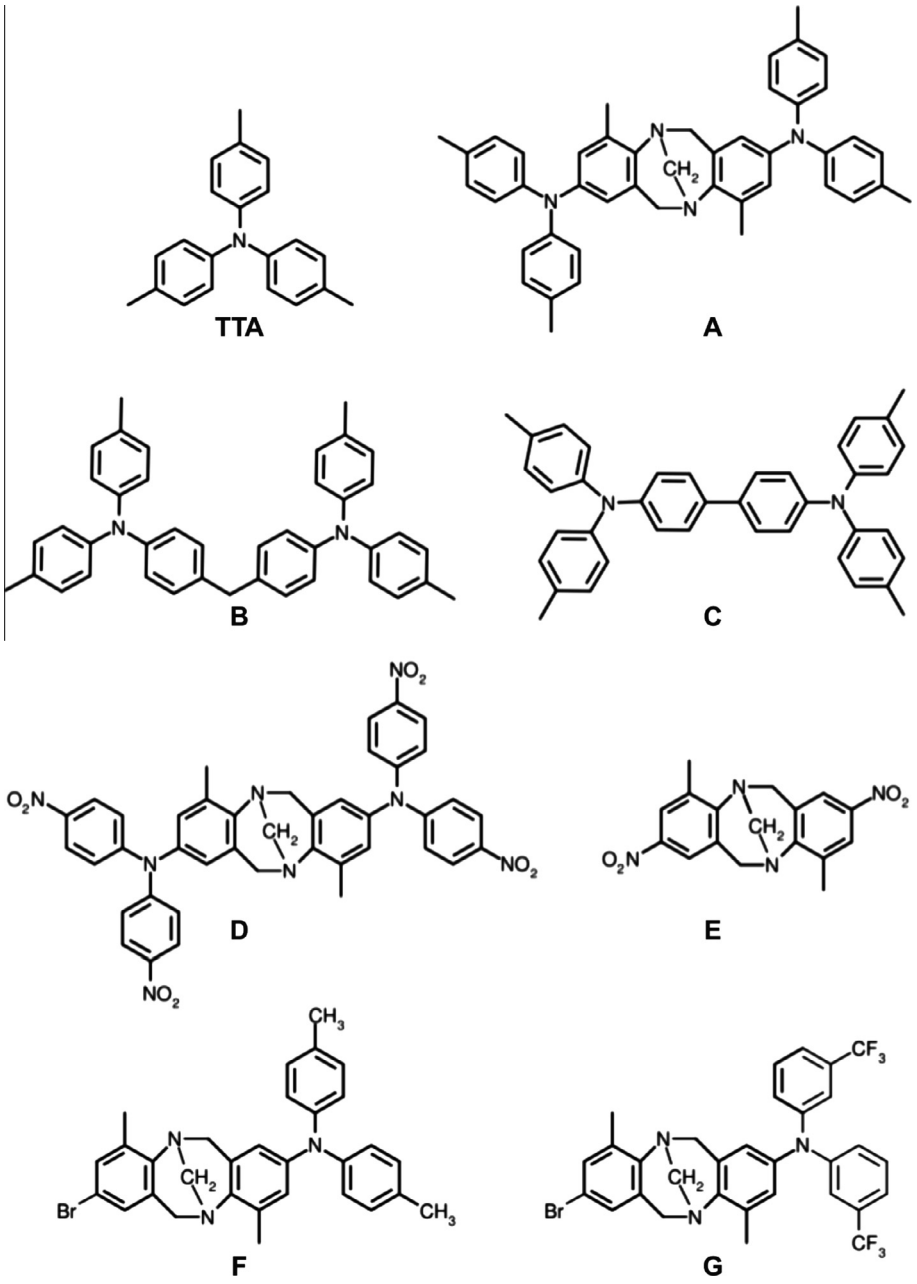

Scheme 1.

The SM Figs. S8–S10 showing the spin density of excited states were obtained from the relaxed excited state density matrix. As discussed below, the characterization of the very intense intervalence charge transfer band in the NIR for highly coupled systems as **A** and **C** is almost obvious. However, this analysis is useful for those spectra where this charge transfer band is hard to detect by experimental means due to both its very low intensity and its possible proximity to other transitions in the visible region. It indeed allows us for identify this band as the one with net charge transfer from one redox fragment to the other from those transitions within the same redox center.

All calculations were done using the Gaussian 09 package [29]. The VMD 1.8.9 [30] program was used for graphics rendering.

4. Results and discussion

4.1. Validation of the computational methodology

As it has been shown by us [7] and other workers [31–35], the Coulomb attenuated version of B3LYP suggested by Yanai et al. (CAM-B3LYP) was able to satisfactorily

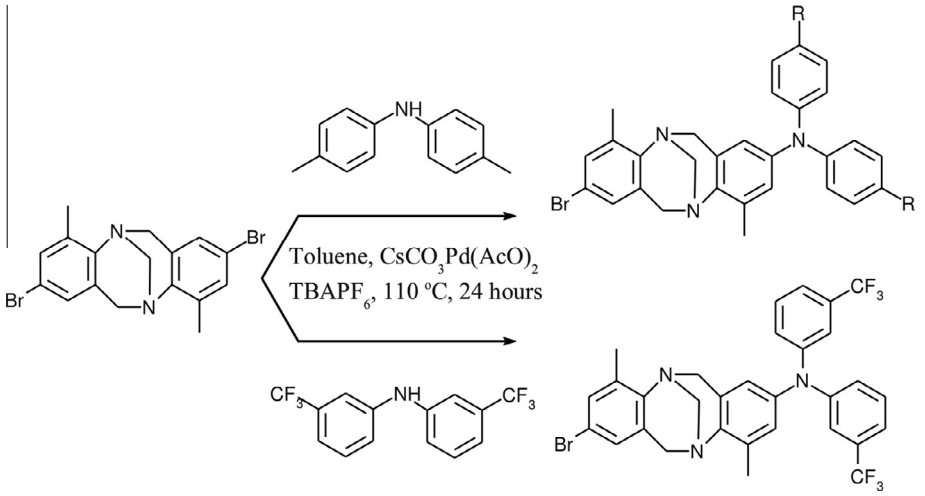

Scheme 2.

Table 1
Summary of predicted and experimental changes in the standard potentials relative to the **TTA**$^{+}$/**TTA** couple.

Compounds	ΔE° (calculated) (V)	ΔE° (experimental) (V)
TTA^{+}/**TTA**[a]	0	0
A^{+}/**A**[a]	0.155	0.160
B^{+}/**B**	0.029	0.030
C^{+}/**C**	−0.075	−0.128[b]
E/**E**$^{-}$	−1.99	−2.06
F^{+}/**F**	−0.060	−0.075
G^{+}/**G**	0.292	0.277

[a] From Ref. [7].
[b] Experimental value from Ref. [15].

describe systems like these, without the overdelocalization problem of B3LYP and other popular hybrid functionals with no distance dependent Hartree–Fock contribution [36]. Here this approach is combined with 6-31 + G* bases[2] and a continuum solvation model. However and first of all, we carefully checked that this setup would be able to reasonably reproduce the thermochemistry of the single electron oxidation or reduction processes. The results of these tests for all compounds in Scheme 1 for which experimental potentials are available are shown in Table 1. For easiness of comparison, all potentials are referred to the tritolylamine **TTA**$^{\cdot+}$/**TTA** couple set as zero, by definition.

At this point, it is worth to note that some coarse effects such as the presence of powerful electron withdrawing groups (as in the case of **G** against either **F** or **TTA**), which facilitate the reduction and turn harder the oxidation, would be easy to predict, even at Koopman's Theorem level.[3] However, finer effects as those arisen from the changes in the localization or delocalization of the oxidized/reduced open shell species are far from being trivial. For example, by comparing the oxidation potential of the methylene-bridged compound **B** to the reference **TTA**, it is clear that the role of certain delocalization (although slight) is to lower the gas phase ionization potential by 140 meV, but in solution there are other electrostatic and non-electrostatic terms which determines the potential. For example, the contribution to the electrostatic solvation is more negative (stabilizing) as the charge localization increases, but the trend is less clear due to the change in the solute volume which is related to the entropy of cavitation and the increase of the solvent accessible area which are both non-electrostatic terms [37]. As a result of all these factors playing together, the shift of **B**$^{\cdot+}$/**B** with respect to **TTA**$^{\cdot+}$/**TTA** is very small and positive by 29 mV (30 ± 10 mV experimental). The details regarding the whole thermodynamic cycle and its components are available as SM Table S1.[4] As another example, the charge delocalization (as it will be discussed later) is comparable in benzidine radical cation (**C**$^{\cdot+}$) and in **A**$^{\cdot+}$, but in the latter case the bridge itself can hold charge in the oxidized species; on the other hand, the shape of the molecule also changes the non-electrostatic terms. Thus, despite the similar difference with respect to **TTA** in the (gas phase) ionization potentials, the solvation of **A**$^{\cdot+}$ is disfavored compared to **C**$^{\cdot+}$ (the $\Delta\Delta G^{\circ}_{solv}$[5] results 150 meV more negative for the latter), it being the main source of difference in the whole shifts. In the case of **F**$^{\cdot+}$, which has the **TTA** moiety bridged to a non-electroactive fragment (the potential of the 2′-methyl-4′-bromophenyl fragment is too far from that of the triarylamine), the shift gathers also a composite of both orbital interactions with one N of the bridge[6] and

[2] This relatively small basis set would be suitable for systems of relatively considerable silze, like these and other system under study in the group.
[3] For example, we checked the correlation at the Koopmans' Theorem level for the HOMOs and the oxidations (not shown), with a standard error of 0.19 V and an R^2 of 0.972 (against 0.02 V and 0.999 respectively, at the current level informed in Table 1).
[4] This SM table also includes the total predicted oxidation or reduction potentials for the cases which were not possible to be determined by experimental means.
[5] The difference between the solvation energy of the oxidized minus the neutral species is indicative of that the redox product formation is favored; see also Ref. [20].
[6] Delocalization shown as spin distribution on SM Fig. S7.

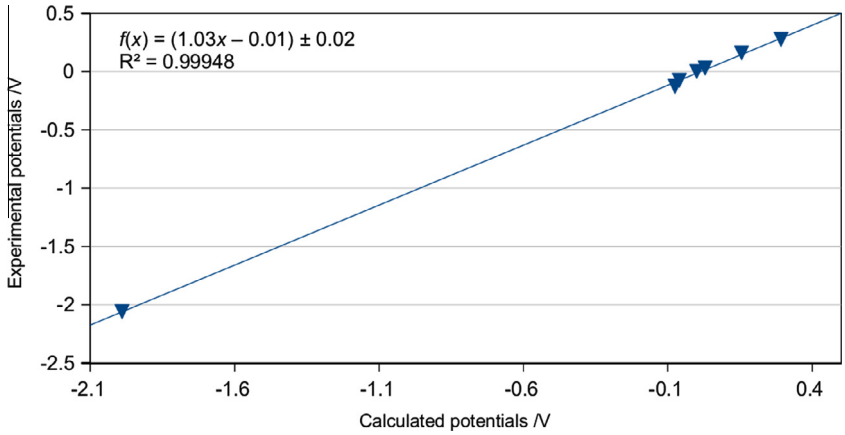

Fig. 1. Correlation between experimental and calculated potentials in main text Table 1 (expressed as reduction couples relative to the **TTA$^+$/TTA** standard potential).

changes in the whole solvation energy of the neutral and cationic species; the net effect being a shift of −60 mV (−75 ± 10 mV experimental).

In sum, in order to reproduce with accuracy the experimental changes in oxidation/reduction potentials of the whole set on Scheme 1, the methodology should be able to describe the actual charge localization/delocalization, to yield accurate adiabatic ionization potentials or electron affinities [38,39] and to achieve a good estimation to the solvation energy of both neutral and charged species. Certainly, this is the case for the level of theory here applied, it featuring a standard error of only 0.02 V as shown in Fig. 1.[7]

4.2. Tröger base bridge in conditions of hole transfer. Comparison to typical π- and σ-linked systems

After validating the predictive capacity of the computational methodology, we continue to compare compound **A** to benzidine (**C**), considered as a paradigmatic case of a fully delocalized intervalence compound (Fig. 2; see also SM Fig. S2). Both the radical cation and the radical anion of **C** bear a single minimum, symmetrically delocalized over the two triarylamine halves, as in the case of the previously reported radical cation of **A** [7]. The electronic description of the oxidized state is also validated by the intense and wide peak of the charge transfer (intervalence) band of the radical cation which was calculated in the NIR at 0.73 eV against 0.85 eV experimental [15] (the intervalence band for **A**$^{\cdot+}$ has been found at 1.14 and 1.36 eV, experimental and TD-DFT respectively [7]; details on the simulated bands and experimental spectra available as SM Figs. S8–S10). Compound **B**, as the simplest and shortest aliphatic bridge was also compared to **A** previously in terms of its EPR spectra, which showed just a slight delocalization of the hole at room temperature, in good agreement to the simulated spin density [7]. In order to asses a comparative measurement of the coupling of the triarylamines with respect to either **A** or **C**, we tried to characterize the (very weak) intervalence band, which was found at nearly 1.46 eV (SM Fig. S9) with an oscillator strength (intensity) at least two orders of magnitude smaller than their highly coupled partners. The transition state for the charge transfer was found at 6.14 kcal/mol, whilst the Marcus-Hush estimate to the diabatic transition state (taken from the optical reorganization energy λ, as $\lambda/4$) was 8.33 kcal/mol. This allows for an estimate to the $2H_{ab}$ matrix element of 760 cm^{-1} (2.2 kcal/mol), which is within the values expected for weakly coupled Type II

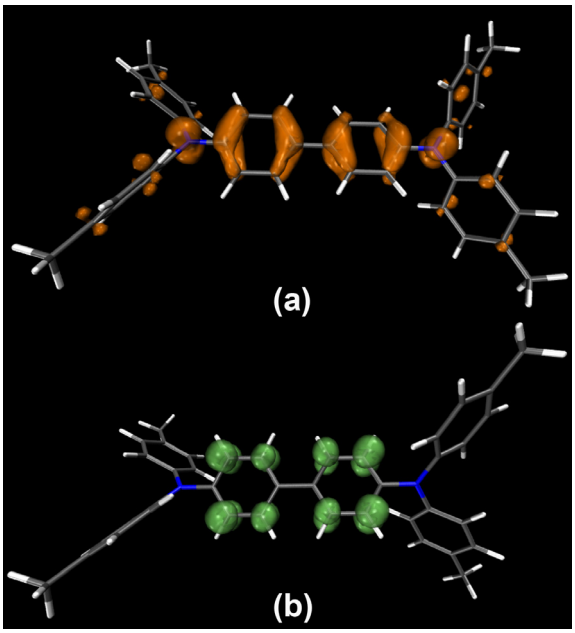

Fig. 2. Spin density isosurfaces (at 0.0025 a.u.) for (a) the radical cation and (b) the radical anion of benzidine (**C**).

[7] Since electron affinities are inherently harder to reproduce than ionization potentials by DFT calculations (see for example Refs. [38,39]), it is also worth to note that the only point obtained in reduction conditions (−1.99 V) could be accurately extrapolated if the linear fit were done by taking only the experimental points in oxidation conditions (−0.1 to +0.4 V range); further details as SM Fig. S1.

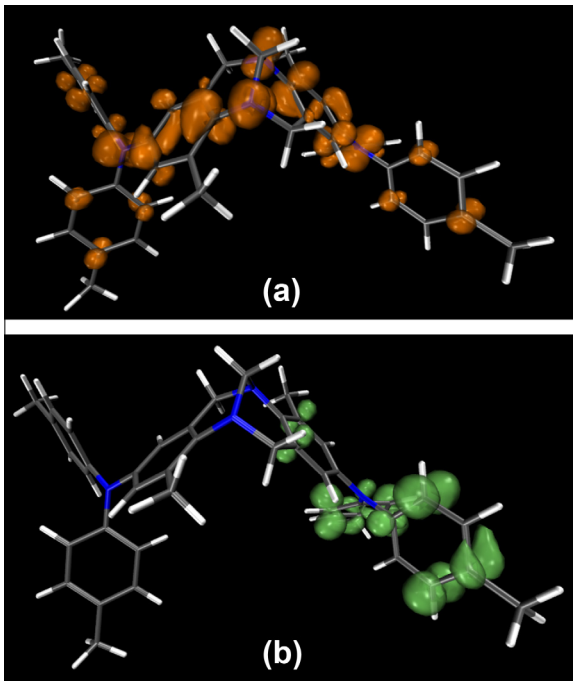

Fig. 3. Spin density for (a) the radical cation of **A** (reproduced from Ref. [7]) and (b) the radical anion of **A**.

intervalence metal complexes [40] (details summarized as SM Fig. S7).

Thus $\mathbf{A}^{\cdot+}$, even though it bears a bulkier and more complex aliphatic bridge, clearly behaves as $\mathbf{C}^{\cdot+}$ for the intramolecular coupling of the redox centers, in contrast to the much shorter $-CH_2-$ aliphatic bridge of $\mathbf{B}^{\cdot+}$. These estimates and the comparison to the well known benzidine system reinforces our previous observations (EPR, electrochemistry, UV–vis–NIR) about the highly efficient coupling between the triarylamines centers in the *radical cation* of **A**. However, our calculations on the electronic properties of the *radical anion* of **A** reveals a completely different pattern.

4.3. Tröger base bridge in conditions of electron transfer

The spin distribution due to the extra electron on $\mathbf{A}^{\cdot-}$ is qualitatively different. As shown in Fig. 3, and in sharp contrast to the radical cation, which was found to delocalize the *hole* all over the molecule [7], the extra *electron* localizes on one center and we were unable to find a transition state for the intramolecular electron transfer from one fragment to the other. For experimental validation, we decided not to go ahead with this compound, due to its very low electron affinity and the resulting difficulties for its reduction (predicted to reduce at −4.55 V against our reference; it being outside the solvent window).[8] Then we calculated two compounds, **D** and **E**, which were expected to be much easier to reduce in dichloromethane due to the presence of the nitro- substituents. Since the radical anions of both compounds showed the same localized pattern as $\mathbf{A}^{\cdot-}$, and also similar calculated reduction potentials among them (see Footnote 8), we choose to continue with **E**, due to its smaller size (computational convenience) and synthetic accessibility.[9]

The radical anion of **E** was found to have three different orbital isomers, two for which the extra electron is localized in one of each nitrophenyl moieties and a symmetrical species which was characterized as a shallow minimum (Fig. 4). We found a considerable difference in energy between the symmetric and asymmetric species, the latter being the most stable by 11.65 kcal/mol.

Both the electrochemistry (Fig. 5) and spectroelectrochemistry (SM Fig. S10) experiments reveal a nearly negligible coupling between the redox centers, again in sharp contrast to the behavior demonstrated by the bridge for the hole transfer. (We also calculated the radical cation of **E**, which features a single totally and symmetrically delocalized minimum as well as $\mathbf{A}^{\cdot+}$, details as SM Fig. S5).[10] The voltammogram for the reduction of **E** (shown in Fig. 5, together with the $\mathbf{TTA}^{\cdot+}/\mathbf{TTA}$ as internal reference) corresponds to a typical uncoupled (or just slightly coupled) system, featuring a single pseudo-reversible reduction wave at −2.06 V from the reference. This peak has no splitting, in contrast to the splitting of around 80–150 mV observed in the coupled partners **A** and **C** [7,15]. The thermochemistry simulated by our calculations is in close agreement to the experimental potential (−1.99 against −2.06 V relative to $\mathbf{TTA}^{+}/\mathbf{TTA}$; Table 1). The spectroelectrochemistry showed practically no intervalence band for this radical anion except for a barely detectable peak in the *visible region* at ~670 nm (1.85 eV). The simulated spectra (TD-DFT) only features a doublet–doublet charge transfer band between the fragments at 595 nm, with a very low oscillator strength (0.01; SM Fig. S10 features the UV–vis–NIR spectra and the spin distribution of this SOMO–LUMO transition). Due to the spectral measurement error and the inherent error of TD-DFT (less accurate than ground state DFT) this charge transfer band could not be unambiguously attributed to the very weak experimental peak. Even if this were not the case, the conclusion is that both theory and experiments find for this radical anion either no charge transfer band or an extremely weak one in the visible, in sharp contrast to the strong and wide intervalence band predicted and experimentally found in the NIR for the radical cation of **A** [7]. The sole existence of the barrier of 12 kcal/mol for reaching the symmetrical state (see Fig. 4) turns the electron transfer between the two aromatics very unlikely.[11] An estimate from Marcus-Hush theory to the barrier for the interconversion, and ignoring the further complication that the system is a three states one, the barrier would be above 12 kcal/mol. Thus, comparing the pairs $\mathbf{A}/\mathbf{A}^{\cdot-}$ and $\mathbf{E}/\mathbf{E}^{\cdot-}$ against $\mathbf{A}^{\cdot+}/\mathbf{A}$ and $\mathbf{E}^{\cdot+}/\mathbf{E}$, the same

[8] Details in the SM Table S1.

[9] Details regarding the calculations on $\mathbf{D}^{\cdot-}$ (not synthesized) on SM Tables S1–2 and Fig. S5.

[10] $\mathbf{E}^{\cdot+}$ is practically impossible to be generated in dichloromethane due to the oxidation potential of **E**, thus the oxidation was not studied experimentally; details on the electronic properties of its radical cation available as SM Fig. S5.

[11] The exact value for the electron transfer intrinsic barrier and the off diagonal matrix element is currently being characterized by multi-reference MCSCF as part of a work in progress.

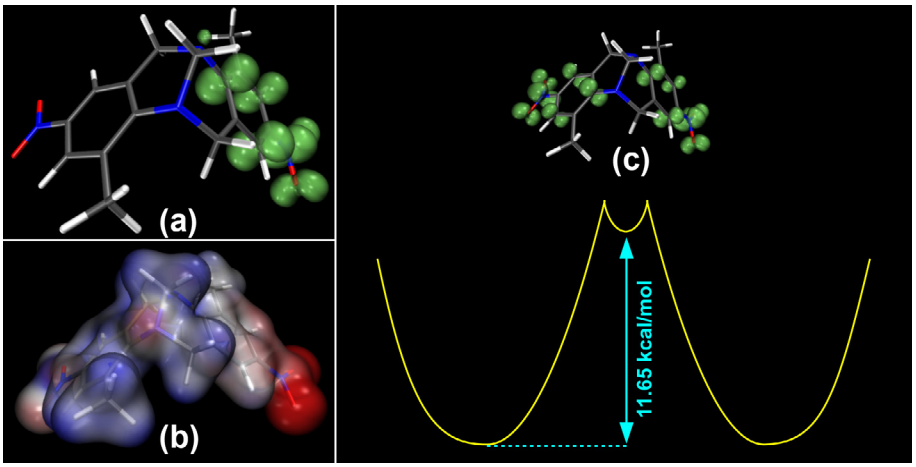

Fig. 4. Main properties of $\mathbf{E}^{-}$. (a) Spin density isosurface (at 0.003 a.u.) (b) electrostatic potential colored from red to blue (−0.2 to +0.1 a.u) on a isodensity surface of 0.02 a.u. (c) Reaction profile for the interchange, showing the spin density on the symmetrical intermediate structure. (For interpretation of the references to colour in this figure legend, the reader is referred to the web version of this article.)

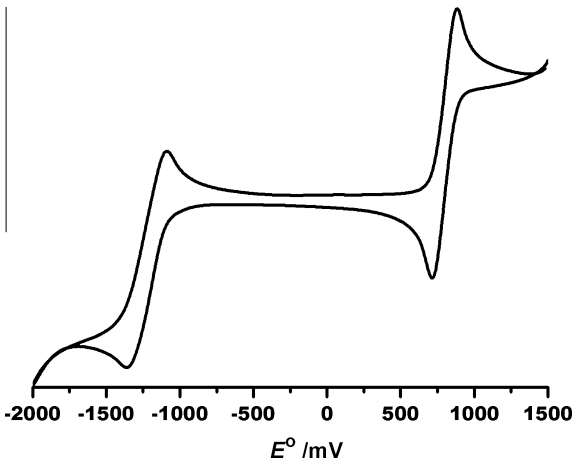

Fig. 5. Voltammogram showing the **E**/$\mathbf{E}^{-}$ and $\mathbf{TTA}^{+}$/**TTA** waves.

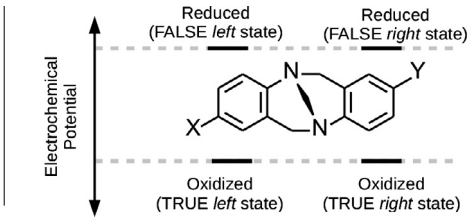

Left	Conduction	Right
TRUE (oxidized)	YES	TRUE (oxidized)
TRUE (oxidized)	YES	FALSE (reduced)
FALSE (reduced)	YES	TRUE (oxidized)
FALSE (reduced)	NO	FALSE (reduced)

Fig. 6. Schematic representation of the HOMO/LUMO levels for donor/bridge/acceptor system based on the bridge under study. If an extra electron goes to the higher level (set as FALSE) the charge transfer is disfavored, yielding the corresponding table of truth shown below.

bridge makes almost impossible the ***electron*** transfer between the different reduced fragments at room temperature whilst, as previously shown, the ***hole***, could be easily interchanged with no activation [7].

4.4. The behavior of the Tröger bridge against electron and hole transport: sharp contrast and its consequences

These charge transfer properties allow for thinking novel functionalities of the Tröger base bridge in combination with the appropriate donor/acceptor edges (for example, arylamines) or conductive contact potential as logical states. By defining the TRUE value as the single electron oxidation potential of any arylamine and FALSE as the reduction one (together with a small bias value set in the case of the same logical state on both sides), the combination of potentials at the left-arylamine and at the right-arylamine of the gate (the Tröger bridge) yield a table of truth for the electric conduction shown in Fig. 6, which corresponds to an OR logic gate. No conduction is possible if both logic states are set to FALSE (i.e. both edges at the reduction potential plus a small bias to induce conduction) since the Tröger bridge does not couple the redox centers for the *electron transfer*. However, if at least one edge is set to TRUE potential, conduction will be possible as the redox centers are efficiently coupled for the *hole transfer* through the aliphatic bonding framework of the bridge.

5. Conclusion

Note that in a typical π bridge, most orbitals have *a priori* the appropriate symmetry for coupling the redox centers either for the hole or electron interaction while, in contrast, an aliphatic bridge usually does not have any. The strained aliphatic Tröger bridge looks special because it fortuitously features a bonding orbital set bearing one which allow for an efficient coupling, but just for holes.

We have already explained in a previous work the role of the nitrogen lone pair as well as the orientation and rigidity of this bridge [7]. With this clue on mind, the rational design of novel single molecular (or supramolecular) applications would be matter of setting the HOMO or LUMO by finding a convenient synthesis of the edges, either arylamine or any aromatic fragment, featuring the desired redox potentials.

Acknowledgments

This work was supported in part by the *Consejo Nacional de Investigaciones Científicas y Tecnológicas* (CONICET), the *Agencia Nacional de Promoción Científica y Tecnológica* (ANPCYT) and *Universidad Nacional de Mar del Plata*. C.L.R. thanks for a CONICET Postdoctoral fellowship. A.R.P. and D.M.A.V. are staff members of CONICET. We gratefully acknowledge the suggestions from Prof. A. Lutzen and from Prof. S. Sergeyev which help us in the synthesis of compound **E** and **F** and **G,** respectively.

Appendix A. Supplementary material

Supplementary data associated with this article can be found, in the online version, at http://dx.doi.org/10.1016/j.orgel.2013.06.024.

The material is a single PDF organized as follows:

Part 1. Electronic properties (electrostatic potentials, spin distribution) of main open shell species. Details on the calculations including total energies and ZPE corrections, details on the thermochemistry of the oxidation/reduction cycles for Table 1. Details on the correlation between experimental and calculated potentials. Calculated properties of the charge transfer excited states and experimental spectroelectrochemistry.

Part 2. Details on the substances characterization.

Part 3. XYZ coordinates of main structures calculated.

References

[1] M. Touraj, R. Sohrab, Synthesis and analysis of triphenylamine: a review, Can. J. Chem. Eng. 82 (2004) 323–334.
[2] Z. Li, H. Meng, Organic Light-emitting Materials and Devices, Taylor & Francis, Group, 2007.
[3] K. Srinivas, G. Sivakumarb, C.R. Kumar, M.A. Reddy, K. Bhanuprakash, V.J. Raob, C.-W. Chen, Y.C. Hsu, J.T. Lin, Novel 1,3,4-oxadiazole derivatives as efficient sensitizers for dye-sensitized solar cells: a combined experimental and computational study, Synth. Met. 161 (2011) 1671–1681.
[4] C. Tai, Y.J. Chen, H.W. Chang, P.L. Yeh, B.C. Wang, DFT and TD-DFT investigations of metal-free dye sensitizers for solar cells: effects of electron donors and π-conjugated linker, Comput. Theor. Chem. 971 (2011) 42–50.
[5] L.M. Peter, The gratzel cell: where next?, J Phys. Chem. Lett. 2 (2011) 1861–1867.
[6] J. Hankache, O.S. Wenger, Organic mixed valence, Chem. Rev. 111 (2011) 5138–5178.
[7] C.L. Ramirez, L. Trupp, A. Bruttomesso, V.T. Amorebieta, D.M.A. Vera, A.R. Parise, Charge transfer properties of Tröger base derivatives, Phys. Chem. Chem. Phys 13 (2011) 20076–20080.
[8] M. Gervaldo, M. Funes, J. Durantini, L. Fernandez, F. Fungo, L. Otero, Electrochemical polymerization of palladium (II) and free base 5,10,15,20-tetrakis(4-N, N-diphenylaminophenyl)porphyrins: Its applications as electrochromic and photoelectric materials, Electrochim. Acta 55 (2010) 1948–1957.
[9] J. Durantini, L. Otero, M. Funes, E.N. Durantini, F. Fungo, M. Gervaldo, Electrochemical oxidation-induced polymerization of 5,10,15,20-tetrakis[3-(N-ethylcarbazoyl)]porphyrin. Formation and characterization of a novel electroactive porphyrin thin film, Electrochim. Acta 56 (2011) 4126–4134.
[10] J. Durantini, G.M. Morales, M. Santo, M. Funes, E.N. Durantini, F. Fungo, T. Dittrich, L. Otero, M. Gervaldo, Synthesis and characterization of porphyrin electrochromic and photovoltaic electropolymers, Org. Electron. 13 (2012) 604–614.
[11] S. Sergeyev, Recent developments in synthetic chemistry, chiral separations, and applications of Troger's base analogues, Helv. Chim. Acta 92 (2009) 415–444.
[12] B. Dolensky, J. Elguero, V. Kral, C. Pardo, M. Valík, Adv. Heterocycl. Chem. 93 (2007) 1–56. ISBN: 978-0-12-373934-6.
[13] C.L. Ramírez, A.R. Parise, Solvent resistant electrochromic polymer based on methylene-bridged arylamines, Org. Electron. 10 (2009) 747–752.
[14] C.L. Ramirez, Electric and Electronic Properties of Intervalence Compounds, PhD Thesis, Universidad Nacional de Mar del Plata, 2012.
[15] P.J. Low, M.A.J. Paterson, A.E. Goeta, D.S. Yufit, J.A.K. Howard, J.C. Cherryman, D.R. Tackley, B. Brown, The molecular structures and electrochemical response of "twisted" tetra(aryl)benzidenes, J. Mater. Chem. 14 (2004) 2516–2523.
[16] S.F. Nelsen, M.N. Weaver, A.E. Konradsson, J.P. Telo, T. Clark, Electron transfer within 2,7-dinitronaphthalene radical anion, J. Am. Chem. Soc. 126 (2004) 15431.
[17] A.B. Pierini, D.M.A. Vera, Ab initio evaluation of intramolecular electron transfer reactions in halobenzenes and stabilized derivatives, J. Org. Chem. 68 (2003) 9191–9199.
[18] U. Kiehne, T. Weilandt, A. Lutzen, Diastereoselective self-assembly of dinuclear double-stranded helicates from Tröger's base derivatives, Org. Lett. 9 (2007) 1283–1286.
[19] I. Noviandri, K. Brown, D.S. Leming, The decamethylferrocenium/decamethylferrocene redox couple: a superior redox standard to the ferrocenium/ferrocene redox couple for studying solvent effects on the thermodynamics of electron transfer, J. Phys. Chem. B 103 (1999) 6713.
[20] V. Grosso, C. Previtali, C.A. Chesta, D.M.A. Vera, A.B. Pierini, An experimental and theoretical study on the field effects exerted by a monopole on the donor-acceptor properties of aromatic systems, Phys. Chem. Chem. Phys. 9 (2007) 5988–5996.
[21] M.T. Cancès, B. Mennucci, J. Tomasi, A new integral equation formalism for the polarizable continnum model: theoretical background and applications to isotropic and anisotropic dielectrics, J. Chem. Phys. 107 (1997) 3032.
[22] B. Mennucci, J. Tomasi, Continuum solvation models: a new approach to the problem of solute's charge distribution and cavity boundaries, J. Chem. Phys. 106 (1997) 5151.
[23] B. Mennucci, E. Cancès, J. Tomasi, Evaluation of solvent effects in isotropic and anisotropic dielectrics and in ionic solutions with a unified integral equation method: theoretical bases, computational implementation, and numerical applications, J. Phys. Chem. B 101 (1997) 10506.
[24] J. Tomasi, B. Mennucci, E. Cancès, The IEF version of the PCM solvation method: an overview of a new method addressed to study molecular solutes at the QM ab initio level, J. Mol. Struct. Theochem. 464 (1999) 211.
[25] D.M. Chipman, Reaction field treatment of charge penetration, J. Chem. Phys. 112 (2000) 5558.
[26] E. Cancès, B. Mennucci, Comment on "Reaction field treatment of charge penetration", J. Chem. Phys. 114 (2001) 4744.
[27] M. Cossi, V. Barone, Time-dependent density functional theory for molecules in liquid solutions, J. Chem. Phys. 115 (2001) 4708.
[28] R. Improta, V. Barone, G. Scalmani, M.J. Frisch, A state-specific polarizable continuum model time dependent density functional theory method for excited state calculations in solution, J. Chem. Phys. 125 (2006). 054103: 1–9.
[29] Gaussian 09, Revision A.01, M.J. Frisch, G.W. Trucks, H.B. Schlegel, G.E. Scuseria, M.A. Robb, J. R. Cheeseman, G. Scalmani, V. Barone, B. Mennucci, G.A. Petersson, H. Nakatsuji, M. Caricato, X. Li, H.P. Hratchian, A.F. Izmaylov, J. Bloino, G. Zheng, J.L. Sonnenberg, M. Hada, M. Ehara, K. Toyota, R. Fukuda, J. Hasegawa, M. Ishida, T. Nakajima, Y. Honda, O. Kitao, H. Nakai, T. Vreven, J.A. Montgomery, Jr., J.E. Peralta, F. Ogliaro, M. Bearpark, J.J. Heyd, E. Brothers, K.N. Kudin, V.N. Staroverov, R. Kobayashi, J. Normand, K. Raghavachari, A. Rendell, J.C. Burant, S.S. Iyengar, J. Tomasi, M. Cossi, N. Rega, J.M. Millam, M. Klene, J.E. Knox, J.B. Cross, V. Bakken, C. Adamo, J. Jaramillo, R. Gomperts, R.E. Stratmann, O. Yazyev, A.J. Austin, R. Cammi, C. Pomelli, J.W. Ochterski, R.L. Martin, K. Morokuma, V.G. Zakrzewski, G.A. Voth, P. Salvador, J.J. Dannenberg, S. Dapprich, A.D.

Daniels, O. Farkas, J.B. Foresman, J.V. Ortiz, J. Cioslowski, D.J. Fox, Gaussian, Inc., Wallingford CT, 2009.
[30] W. Humphrey, A. Dalke, K. Schultten, J. Mol. Graphics 14 (1996) 33. <http://www.ks.uiuc.edu/Research/vmd/>.
[31] T. Heaton-Burgess, W. Yang, Structural manifestation of the delocalization error of density functional approximations: C4N+2 rings and C20 bowl, cage, and ring isomers, J. Chem. Phys. 132 (2010) 234113.
[32] Z.L. Cai, M.J. Crossley, J.R. Reimers, R. Kobayashi, R.D. Amos, Density-functional theory for charge-transfer: the nature of the N-bands of porphyrins and chlorophylls revealed through CAM-B3LYP, CASPT2, and SAC-CI calculations, J. Phys. Chem. B 110 (2006) 15624–15632.
[33] I.V. Rostov, R.D. Amos, R. Kobayashi, G. Scalmani, M.J. Frisch, Studies of the ground and excited-state surfaces of the retinal chromophore using CAM-B3LYP, J. Phys. Chem. B 114 (2010) 5547–5555.
[34] F. Maurel, A. Perrier, D. Jacquemin, An ab initio simulation of a dithienylethene/phenoxynaphthacenequinone photochromic hybrid, J. Photochem. Photobiol. A. Chem. 218 (2011) 33–40.
[35] L. Ferrighia, L. Frediania, C. Cappellib, P. Salekc, H. Agrenc, T. Helgakerd, K. Ruud, Density-functional-theory study of the electric-field-induced second harmonic generation (EFISHG) of push–pull phenylpolyenes in solution, Chem. Phys. Lett. 425 (2006) 267–272.
[36] T. Yanai, D.P. Tew, N.C. Handy, A new hybrid exchange–correlation functional using the Coulomb-attenuating method (CAM-B3LYP), Chem. Phys. Lett. 393 (2004) 51–57.
[37] J. Tomasi, B. Mennucci, R. Cammi, Quantum mechanical continnum solvation models, Chem. Rev. 105 (2005) 2999–3093.
[38] J.C. Rienstra-Kiracofe, G.S. Tschumper, H.F. Schaefer III, S. Nandi, G.B. Ellison, Atomic and molecular electron affinities: photoelectron experiments and theoretical computations, Chem. Rev. 102 (2002) 231–282.
[39] D.M.A. Vera, A.B. Pierini, Species with negative electron affinity and standard DFT methods, Phys. Chem. Chem. Phys. 6 (2004) 2899–2903.
[40] J.E. Sutton, P.M. Sutton, H. Taube, Determination of the comproportionation constant for a weakly coupled mixed-valence system by titration of the intervalence transfer band:mu.-(4,4'-bipyridyl)-bis(pentaammineruthenium)(5+), Inorg. Chem. 18 (1979) 1017–1021.